with a 95% confidence interval of 9.0–33.8% (Table 2). Fungal cultures of the nondirected BAL yielded positive results in seven (77.8%) patients with IPA and only one (3%) patient without IPA, who, because of lack of clinical deterioration and lack of increased BAL GM levels, was ruled to be colonized with *Aspergillus*. At 30-day follow-up after inclusion cessation, ICU mortality in the IPA group was 22.2% and 15.1% in the non-IPA group ($P = 0.61$). Autopsies were not performed because of a perceived risk of contamination. Mean ICU length of stay was 37 days for patients with IPA versus 19 for those without IPA ($P < 0.05$).

A bronchoscopy with BAL is the preferred diagnostic approach because GM antigen detection and culture have a good sensitivity in influenza-associated IPA. However, given the risk of aerosolization, The American Association for Bronchology and Interventional Pulmonology issued a statement providing a limited role for bronchoscopy in patients with COVID-19, advocating the use of a nonbronchoscopic alveolar lavage (10). The technique we used in this study minimizes the risk for care providers while providing a diagnostic tool for our patients. However, the nondirected BAL technique is not validated for GM detection. As all patients had consolidations in all regions of the lung, the chances that a nondirected BAL may result in sampling of a lung region that was not affected by IPA may be low, although it is unclear to which extent consolidations are caused by the virus or by the fungus. More importantly, we cannot rule out overdiagnosis, as a nondirected sample may not always reflect microbiology of the lower airways. Therefore, instead of 0.5, a cutoff GM index of 1.0 was applied in this study. Nevertheless, sampling error cannot be ruled out. Of note, however, concordance between GM index >1.0 and positive *Aspergillus* cultures was high (77.8%).

Early detection and treatment of IPA improves outcome compared with delayed diagnosis. Therefore, we opted to treat all nine patients who were deemed to have putative IPA with antifungal therapy (with an empirical regimen consisting of amphotericin B and voriconazole). We noted a longer ICU length of stay for patients who developed IPA, although ICU mortality did not differ between groups. However, whether COVID-19–associated IPA contributes to mortality, or whether IPA therapy improves outcome, cannot be dissected from our study.

We conclude that the incidence of putative IPA may be high in patients with COVID-19 and that chronic obstructive pulmonary disease may be a particular risk factor. Implementation of surveillance of mechanically ventilated patients with COVID-19 using the nondirected BAL technique is feasible. As COVID-19–associated IPA appears to resemble influenza-associated IPA in many ways, and ICU length of stay was longer in those with IPA versus those without, it is our opinion that active surveillance and treatment may be beneficial in patients with COVID-19. ■

Author disclosures are available with the text of this letter at www.atsjournals.org.

Stefaan Van Biesen, M.D.
David Kwa, M.D., Ph.D.
Robert J. Bosman, M.D.
OLVG Hospital
Amsterdam, the Netherlands

Nicole P. Juffermans, M.D., Ph.D.*
OLVG Hospital
Amsterdam, the Netherlands
and
Amsterdam University Medical Center
Amsterdam, the Netherlands

*Corresponding author (e-mail: n.p.juffermans@amsterdamumc.nl).

References

1. Vanderbeke L, Spriet I, Breynaert C, Rijnders BJA, Verweij PE, Wauters J. Invasive pulmonary aspergillosis complicating severe influenza: epidemiology, diagnosis and treatment. *Curr Opin Infect Dis* 2018;31: 471–480.
2. Patterson TF, Thompson GR III, Denning DW, Fishman JA, Hadley S, Herbrecht R, *et al*. Practice guidelines for the diagnosis and management of aspergillosis: 2016 update by the Infectious Diseases Society of America. *Clin Infect Dis* 2016;63:e1–e60.
3. Koehler P, Cornely OA, Böttiger BW, Dusse F, Eichenauer DA, Fuchs F, *et al*. COVID-19 associated pulmonary aspergillosis. *Mycoses* 2020; 63:528–534.
4. van Arkel ALE, Rijpstra TA, Belderbos HNA, van Wijngaarden P, Verweij PE, Bentvelsen RG. COVID-19-associated pulmonary aspergillosis. *Am J Respir Crit Care Med* 2020;202:132–135.
5. Alanio A, Dellière S, Fodil S, Bretagne S, Mégarbane B. High prevalence of putative invasive pulmonary aspergillosis in critically ill COVID-19 patients. *SSRN Electron J* [online ahead of print] 15 Apr 2020; DOI: 10.2139/ssrn.3575581.
6. Lahmer T, Rasch S, Spinner C, Geisler F, Schmid RM, Huber W. Invasive pulmonary aspergillosis in severe coronavirus disease 2019 pneumonia. *Clin Microbiol Infect* [online ahead of print] 2 Jun 2020; DOI: 10.1016/j.cmi.2020.05.032.
7. Rutsaert L, Steinfort N, Van Hunsel T, Bomans P, Naesens R, Mertes H, *et al*. COVID-19-associated invasive pulmonary aspergillosis. *Ann Intensive Care* 2020;10:71.
8. Verweij PE, Gangneux JP, Bassetti M, Brüggemann RJM, Cornely OA, Koehler P, *et al*. Diagnosing COVID-19-associated pulmonary aspergillosis. *Lancet Microbe* [online ahead of print] 8 May 2020; DOI: 10.1016/ S2666-5247(20)30027-6.
9. Blot SI, Taccone FS, Van den Abeele AM, Bulpa P, Meersseman W, Brusselaers N, *et al*.; AspICU Study Investigators. A clinical algorithm to diagnose invasive pulmonary aspergillosis in critically ill patients. *Am J Respir Crit Care Med* 2012;186:56–64.
10. Wahidi MM, Lamb C, Murgu S, Musani A, Shojaee S, Sachdeva A, *et al*. American Association for Bronchology and Interventional Pulmonology (AABIP) statement on the use of bronchoscopy and respiratory specimen collection in patients with suspected or confirmed COVID-19 infection. *J Bronchology Interv Pulmonol* [online ahead of print] 18 Mar 2020; DOI: 10.1097/LBR.0000000000000681.

High Respiratory Drive and Excessive Respiratory Efforts Predict Relapse of Respiratory Failure in Critically Ill Patients with COVID-19

Since the first reported cases in December 2019 in Wuhan, China, coronavirus disease (COVID-19) outbreak has rapidly spread

Author Contributions: P.E., M.C., and C.G. contributed to the study concept and design. P.E., M.C., P.G., E.P'h., and C.G. contributed to the acquisition of data. P.E., S.H., P.G., K.B., and C.G. contributed to the analysis and interpretation of data. P.E., J.B., J.M.-F., E.M., L.P., and C.G. contributed to drafting the manuscript and critically revising the manuscript for important intellectual content. All authors read and approved the final manuscript.

This letter has a related editorial.

Originally Published in Press as DOI: 10.1164/rccm.202005-1582LE on August 5, 2020

around the world (1). This infection often requires ICU admissions and invasive mechanical ventilation (2). To prevent diaphragmatic atrophy and to enhance weaning, the early use of ventilatory modes allowing spontaneous breathing is usually recommended as soon as possible but should be balanced with potential harmful effects. Indeed, a high respiratory drive is sometimes observed in patients with acute respiratory distress syndrome (ARDS), and thus, spontaneous breathing could lead to uncontrolled transpulmonary pressures and possibly to patient self-inflicted lung injuries (P-SILI) (3, 4). Strong efforts could also simply reflect the nonresolution of the underlying disease and thus invite to delay the weaning process of mechanical ventilation. Lacking specific respiratory monitoring, surrogate measures of respiratory drive should be assessed. Airway occlusion pressure ($P_{0.1}$) is a simple, noninvasive measurement method for estimating respiratory drive during mechanical ventilation (3, 5). It is automatically available in almost all ventilators. $P_{0.1}$ is the negative airway pressure generated during the first 100 ms of an occluded inspiration. Because of the very short duration and zero flow, it is independent from respiratory muscle weakness as well as respiratory system compliance and resistance. However, it provides little information about the magnitude of dynamic lung stress (5, 6). It has been proposed to target a range between 1.5 and 3.5 cm H_2O of $P_{0.1}$ (3). The airway pressure deflection generated by the patient's respiratory effort during an end-expiratory airway occlusion (ΔPocc) is a recently validated noninvasive technique for detecting excessive respiratory effort and dynamic lung stress during assisted mechanical ventilation (6). Bertoni and colleagues showed that measurements of ΔPocc allow a reliable and bedside estimation of respiratory muscle pressure (Pmus) by using a conversion factor (predicted $Pmus = -0.75 \times \Delta Pocc$) (6). Besides, in a recent editorial, Gattinoni and colleagues suggested that $P_{0.1}$ and ΔPocc should be determined in patients with COVID-19 to assess excessive inspiratory efforts (7). The validity of $P_{0.1}$ or ΔPocc measurements in intubated and mechanically ventilated patients with COVID-19 has not been evaluated.

We hypothesized that mechanically ventilated patients with COVID-19 with ARDS often present high respiratory drive and excessive inspiratory efforts (as suggested by elevated $P_{0.1}$ and ΔPocc measurements) and that this could rapidly lead to a relapse of respiratory failure during the weaning process of mechanical ventilation.

Therefore, the aim of this study was to assess the threshold values of $P_{0.1}$ and ΔPocc predicting the occurrence of relapse in the following 24-hour period after measurements in intubated and mechanically ventilated patients with COVID-19 pneumonia.

Methods

We conducted a retrospective, bicenter study at the Sainte Anne Military Hospital and the Marseille University North Hospital. This study enrolled critically ill patients with mild to severe ARDS due to COVID-19 (positive result of a real-time RT-PCR assay in nasal or pulmonary samples), intubated and mechanically ventilated, in supine position, and with spontaneous breathing (pressure support ventilation [PSV] or airway pressure release ventilation [APRV]).

The study was approved by the institutional review board of the Sainte Anne Military Hospital (no. 0011873-2020-05), which waived the requirement for informed consent from patients and their relatives, given the retrospective and observational nature of the study.

$P_{0.1}$ and ΔPocc measurements were performed by the clinician in charge in each patient on the first day on APRV mode or PSV mode. $P_{0.1}$ was measured at least three times (1 min between each measurement), and the mean $P_{0.1}$ was notified. ΔPocc was defined as the maximal deflection in airway pressure from positive end-expiratory pressure (PEEP) during an end-expiratory airway occlusion (6). Measurements were repeated at least three times, and the highest value was recorded.

Automated measurements were performed with four commercialized ventilators: Evita XL (Dräger), Evita Infinity V500 (Dräger), Avea (CareFusion), and Carescape R860 (GE Healthcare). The accuracy and precision of values of $P_{0.1}$ displayed by these ventilators have been validated (8, 9). The same ventilator was used for a given patient.

The main endpoint of the study was a relapse of respiratory failure during the weaning process of invasive mechanical ventilation in the 24-hour period following measurements defined by the presence of at least one of the following criteria: decrease of Pa_{O_2}/FI_{O_2} ratio ⩾20%, or severe hypoxemia (oxygen saturation as measured by pulse oximetry [Sp_{O_2}] <88% under FI_{O_2} ⩾60% for >15 min), new onset of respiratory acidosis (pH <7.35), or increase of Pa_{CO_2} ⩾10 mm Hg in patients with preceding respiratory acidosis. Ventilator settings were optimized in case of respiratory worsening as follows: 2 cm H_2O stepwise increase of pressure support (PS) until 14 cm H_2O when respiratory rate was >35/min or V_T was <6 ml/kg of predicted body weight (PBW), decrease of PS until 0 cm H_2O or increase of sedation (without loss of spontaneous breathing) in case of V_T >8 ml/kg of PBW, and 2 cm H_2O stepwise increase of PEEP until 16 cm H_2O when Sp_{O_2}/FI_{O_2} was <150 (10). If temporary deoxygenations were observed (e.g., following an accidental ventilator disconnection, airway suctioning, transport to computed tomographic scan) and were not followed by any medical intervention (i.e., change of ventilator settings, increase in sedations), they were not considered a relapse of respiratory failure.

The method of weaning was similar in the two ICUs. Briefly, all patients were initially ventilated in volume-controlled mode. When the Pa_{O_2}/FI_{O_2} ratio was greater than 150 mm Hg during at least 6 hours without neuromuscular blockers, and/or use of prone positioning or inhaled nitric oxide in the last 12 hours, volume-controlled mode was switched to APRV mode (minimal $time_{high}$:$time_{low}$ was 1 s:1.5–2 s, Phigh was set to achieve a V_T of 6–8 ml/kg of PBW with a maximal driving pressure of 15 cm H_2O, Plow was the corresponding PEEP during volume-controlled mode). When spontaneous minute ventilation was above 50% in APRV mode, ventilator settings were switched to PSV. The PS was then decreased every 4 hours if V_T remained ⩾6 ml/kg of PBW and respiratory rate remained <35/min. PEEP was gently (2 cm H_2O stepwise) decreased every 8–12 hours if Pa_{O_2}/FI_{O_2} ratio remained ⩾200 mm Hg. Extubation was considered when PS was ⩽4 cm H_2O with V_T >6 ml/kg of PBW and respiratory rate <35/min, PEEP was ⩽6 cm H_2O, and FI_{O_2} was ⩽40% with Pa_{O_2}/FI_{O_2} ratio ⩾200 mm Hg. A spontaneous breathing trial using a T-tube was not systematically performed before extubation.

Statistical analysis was performed using R software, version 3.5.1 (The R Foundation for Statistical Computing). Nonparametric

variables were compared using a Mann-Whitney test. Abilities of $P_{0.1}$ or ΔPocc to predict a relapse of respiratory failure were represented by a receiver operating characteristic (ROC) curve analysis. Areas under the curves (AUCs) were presented with their 95% confidence interval (95% CI). The diagnostic cutoff was determined by the highest Youden index value. Because some patients underwent several $P_{0.1}$ and ΔPocc measurements, we analyzed only the first values of $P_{0.1}$ and ΔPocc measurements.

Results

Twenty-eight patients with COVID-19 admitted in the two ICUs from March 10 through April 14, 2020, were included. Population characteristics are displayed in Table 1.

A total of 28 paired measurements of $P_{0.1}$ (3 measures, mean value of the 3) and ΔPocc (highest value of 3 measures) were performed (4 on APRV mode and 24 on PSV mode). Time from the onset of invasive mechanical ventilation to first measurements was 8.5 (interquartile range [IQR], 4–12) days. Before measurements, median Richmond Agitation-Sedation Scale was −4 (IQR, −4 to −4). Ventilator settings before measurements were as follows: PS at 6 (IQR, 4–11) cm H_2O, PEEP at 12 (IQR, 10–14) cm H_2O, and V_T of 6.6 (IQR, 6.3–7.3) ml/kg of PBW. Median rapid shallow breathing index was 49 (IQR, 40–62) breaths/min/L. Median minute ventilation was 11.1 (IQR, 8.9–12.6) L/min. Results of last blood gas analysis before measurements were as follows: Pa_{O_2} 83 (IQR, 77–97) mm Hg, Pa_{CO_2} 46.2 (IQR, 39.7–49.3) mm Hg, pH 7.43 (IQR, 7.42–7.46), and Pa_{O_2}/FI_{O_2} ratio 203 (IQR, 187–238) mm Hg.

Mean $P_{0.1}$ value was 4.4 ± 3.0 cm H_2O. Notably, 14 measurements (50%) were >3.5 cm H_2O, and 7 (25%) were ⩾6.0 cm H_2O. Twelve ΔPocc measurements (43%) were <−15 cm H_2O.

Of the 28 measurements, 9 (32%) were followed by a relapse of respiratory failure. As illustrated in the Figure 1, median $P_{0.1}$ were significantly higher in those cases (6.9 [IQR, 4.3 to 9.6] cm H_2O vs. 3 [IQR, 1.6 to 4] cm H_2O), and median ΔPocc were lower (−18 [IQR, −26 to −15] cm H_2O vs. −15 [IQR, −18 to −7] cm H_2O).

One measurement was followed by a successful extubation with a value of $P_{0.1}$ at 3.0 cm H_2O.

ROC curve showed that $P_{0.1}$ had a satisfactory accuracy to predict a relapse with an AUC of 0.84 (95% CI, 0.67–1.00), $P = 0.004$ (Figure 1). The maximum value of the Youden index was obtained for a $P_{0.1}$ ⩾4 cm H_2O. The prognostic performance of this threshold showed a sensitivity of 89% (95% CI, 52–100), a specificity of 74% (95% CI, 49–91), a positive predictive value of 62% (95% CI, 32–86), a negative predictive value of 93% (95% CI, 68–100), a positive likelihood ratio (LR) of 3.38 (95% CI, 1.54–7.42), a negative LR of 0.15 (95% CI, 0.02–0.98), and a diagnostic accuracy of 79% (95% CI, 59–92).

ROC curve demonstrated that ΔPocc had an acceptable accuracy to predict a relapse with an AUC of 0.73 (95% CI, 0.55–0.92), $P = 0.05$ (Figure 1). The maximum value of the Youden index was obtained for a ΔPocc < −10 cm H_2O. The prognostic performance of this threshold showed a sensitivity of 100% (95% CI, 66–100), a specificity of 42% (95% CI, 20–67), a positive predictive value of 45% (95% CI, 23–68), a negative predictive value of 100% (95% CI, 63–100), a positive LR of 1.73 (95% CI, 1.18–2.53), a negative LR of 0.00 (95% CI, 0.00–0.00), and a diagnostic accuracy of 61% (95% CI, 41–78).

Table 1. Baseline Characteristics, Treatments, and Main Outcomes of Included Patients

Demographic data	
Age, yr	66 (57–73)
Sex, M	22 (78.6)
Comorbidities	
Any	25 (89)
⩾3	11 (39)
Arterial hypertension	20 (71)
Diabetes	5 (18)
BMI >25 kg/m^2	9 (32)
Obstructive sleep apnea	7 (25)
Chronic obstructive pulmonary disease	4 (14)
Coronary heart disease	3 (11)
Chronic kidney disease	2 (7)
Malignancy	3 (11)
Time from onset of symptoms to	
ICU admission, d	8 (5–11)
Invasive mechanical ventilation, d	9 (5–11)
SAPS II score at admission	59 (39–65)
SOFA score at admission	7 (4–9)
Minimal Pa_{O_2}/FI_{O_2} ratio, mm Hg	110 (98–128)
Mild ARDS	1 (4)
Moderate ARDS	19 (68)
Severe ARDS	8 (29)
Treatments for ARDS	
Continuous infusion of neuromuscular blockers	24 (86)
Prone position	19 (68)
Inhaled nitric oxide	6 (21)
Almitrine infusion	2 (7)
Extracorporeal membrane oxygenation	1 (4)
Outcomes	
VFD at Day 30	0 (0–5)
Weaning before Day 30	11 (39)
Tracheostomy	17 (61)
Renal replacement therapy	2 (7)
Discharge from ICU before Day 30	11 (39)
30-d mortality	1 (4)

Definition of abbreviations: ARDS = acute respiratory distress syndrome; BMI = body mass index; SAPS II = Simplified Acute Physiology Score; SOFA = Sequential Organ Failure Assessment; VFD = ventilator-free days. $n = 28$. Data are expressed as *n* (%) or median (interquartile range).

Prognostic performances of the other thresholds are presented in Table 2.

Finally, AUC for $P_{0.1}$ was not significantly different than AUC for ΔPocc (DeLong's test, $P = 0.32$).

We then split measurements into four categories: low ΔPocc (⩾−15 cm H_2O)/low $P_{0.1}$ (<4 cm H_2O), high ΔPocc (<−15 cm H_2O)/low $P_{0.1}$, low ΔPocc/high $P_{0.1}$ (⩾4 cm H_2O), and high ΔPocc/high $P_{0.1}$. Proportions of relapse of respiratory failure were, respectively, 0/11 (0%), 1/4 (25%), 3/5 (60%), and 5/8 (62.5%) ($P = 0.015$).

Discussion

In this cohort of patients with COVID-19, we found that $P_{0.1}$ was frequently above 3.5 cm H_2O, suggesting high neural respiratory drive (3, 11). Even if ranges of $P_{0.1}$ up to 6.0 cm H_2O have been reported in patients with ARDS, a quarter of our measurements were above this value (5). $P_{0.1}$ is an easy and reliable tool to measure the respiratory drive, available worldwide. Recently, Telias and colleagues demonstrated that $P_{0.1}$ directly

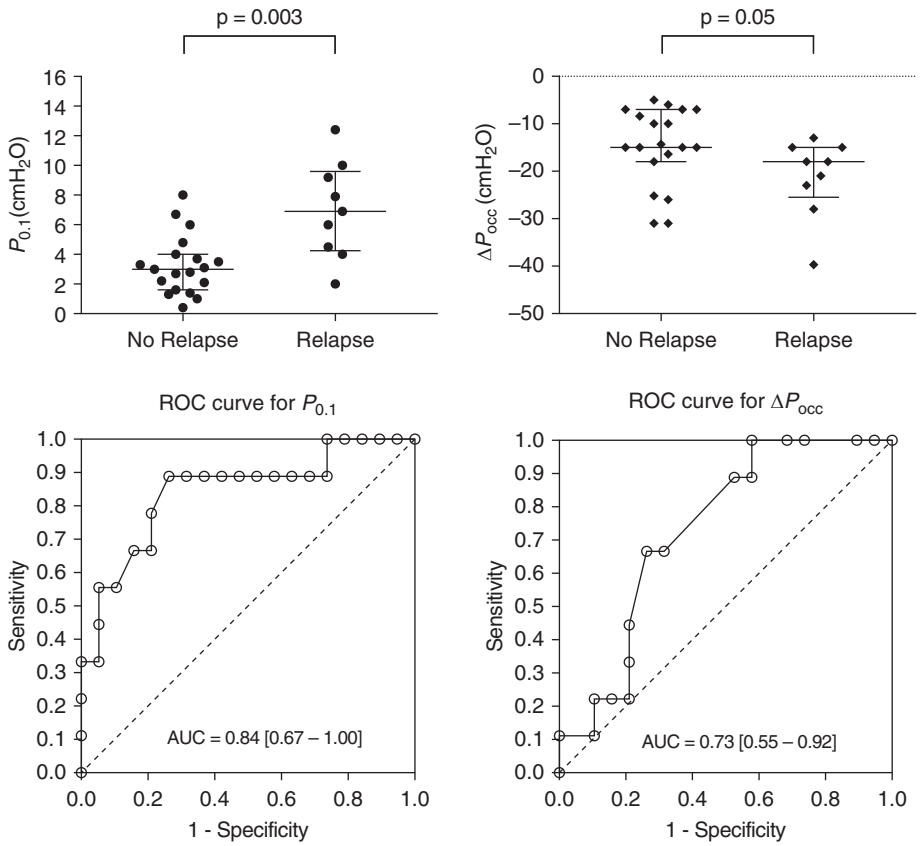

Figure 1. Abilities of airway occlusion pressure ($P_{0.1}$) and end-expiratory airway occlusion (ΔPocc) to predict relapse of respiratory failure during the weaning process of invasive mechanical ventilation. (Top) Scatter dot plots describing $P_{0.1}$ (left) and ΔPocc (right) values (median with interquartile range) followed or not by a relapse. (Bottom) ROC curves of $P_{0.1}$ (left) and ΔPocc (right) for prediction of relapse of respiratory failure. AUC = area under the curve; ROC = receiver operating characteristic.

displayed by the ventilator correlates with invasive measures of respiratory drive (electrical activity of the diaphragm and muscular pressure measured with esophageal pressure). They also showed that $P_{0.1}$ was well correlated with pressure–time product per minute, a surrogate of inspiratory effort (9).

We found that $P_{0.1}$ had a reliable accuracy to predict relapse of respiratory failure in the first 24 hours after measurement of $P_{0.1}$ and ΔPocc in our population. A $P_{0.1}$ $\geq$4.0 cm H_2O had an excellent specificity and negative predictive value. Relapse might be a consequence of P-SILI and myotrauma, or also due to the nonresolution of the COVID-19 pneumonia. High drive and excessive respiratory efforts could possibly lead to P-SILI through different mechanisms such as an excessive global and regional lung stress, a pulmonary edema, or patient–ventilator asynchronies (3). The diaphragm is also sensitive to an excessive respiratory load, ensuing load-induced diaphragm injury (myotrauma).

ΔPocc measurements were also frequently less than -15 cm H_2O, which can correspond, after application of conversion factor, to Pmus greater than 10 cm H_2O, indicating excessive respiratory efforts (6). Indeed, Bertoni and colleagues propose to target a range of Pmus between 5 and 10 cm H_2O during spontaneous breathing (3). Even if ΔPocc was less discriminating than $P_{0.1}$, its regular measurement is also interesting to predict a relapse of respiratory failure during mechanical ventilation weaning. Moreover, we found that high ΔPocc and high $P_{0.1}$ association is at higher risk of relapse of respiratory failure.

This study has several limitations including its retrospective design and the limited number of patients included. A comparative measure of respiratory drive and inspiratory efforts such as electrical activity of the diaphragm or muscular pressure measured with esophageal catheter might have helped to confirm our results.

In conclusion, in this COVID-19 pandemic context, with limited time and material resources, serial measurements of $P_{0.1}$ and ΔPocc could be a valuable bedside clinical tool to predict relapse of respiratory failure in the next 24 hours and therefore to potentially delay the weaning process of mechanical ventilation, especially when $P_{0.1}$ is $\geq$4 cm H_2O and ΔPocc is <-15 cm H_2O. ■

Author disclosures are available with the text of this letter at www.atsjournals.org.

Pierre Esnault, M.D., M.Sc.*
Michael Cardinale, M.D.
Sainte Anne Military Hospital
Toulon, France

Sami Hraiech, M.D., Ph.D.
Assistance Public–Hôpitaux de Marseille (APHM)
Marseille, France
and
Aix-Marseille University
Marseille, France

Table 2. Prognostic Performance of Different Threshold of $P_{0.1}$ and ΔPocc to Predict Relapse of Respiratory Failure during the Weaning Process of Invasive Mechanical Ventilation

Thresholds ($cm\ H_2O$)	Sensitivity (%)	Specificity (%)	PPV (%)	NPV (%)	LR+	LR−	Diagnostic Accuracy (%)	Youden Index
$P_{0.1}$								
⩾3	89 (52–100)	47 (24–71)	44 (22–69)	90 (55–100)	1.69 (1.04–2.74)	0.23 (0.03–1.58)	61 (41–78)	0.36
⩾4	89 (52–100)	74 (49–91)	62 (32–86)	93 (68–100)	3.38 (1.54–7.42)	0.15 (0.02–0.98)	79 (59–92)	0.63
⩾5	67 (30–93)	84 (60–97)	67 (30–93)	84 (60–97)	4.22 (1.36–13.16)	0.40 (0.15–1.02)	79 (59–92)	0.51
⩾6	67 (30–93)	84 (60–97)	67 (30–93)	84 (60–97)	4.22 (1.36–13.16)	0.40 (0.15–1.02)	79 (59–92)	0.51
⩾7	44 (14–79)	95 (74–100)	80 (28–99)	78 (56–93)	8.44 (1.10–65.12)	0.59 (0.32–1.06)	79 (59–92)	0.39
ΔPocc								
<−10	100 (66–100)	42 (20–67)	45 (23–68)	100 (63–100)	1.73 (1.18–2.53)	0.00 (0.00–0.00)	61 (41–78)	0.42
<−15	67 (30–93)	68 (43–87)	50 (21–79)	81 (54–96)	2.11 (0.94–4.73)	0.49 (0.18–1.29)	68 (48–84)	0.35
<−20	44 (14–79)	79 (54–94)	50 (16–84)	75 (51–91)	2.11 (0.68–6.58)	0.70 (0.38–1.32)	68 (48–84)	0.23
<−25	22 (03–60)	79 (54–94)	33 (04–78)	68 (45–86)	1.06 (0.24–4.73)	0.99 (0.65–1.50)	61 (41–78)	0.01
<−30	11 (00–48)	89 (67–99)	33 (01–91)	68 (46–85)	1.06 (0.11–10.17)	0.99 (0.75–1.31)	64 (44–81)	0.00

Definition of abbreviations: ΔPocc = airway pressure deflection generated by respiratory effort during an end-expiratory airway occlusion; LR+ = positive likelihood ratio; LR− = negative likelihood ratio; NPV = negative predictive value; $P_{0.1}$ = airway occlusion pressure; PPV = positive predictive value.
Data in parentheses are 95% confidence intervals.

Philippe Goutorbe, M.D.
Sainte Anne Military Hospital
Toulon, France

Karine Baumstrack, M.D., Ph.D.
APHM
Marseille, France
and
Aix-Marseille University
Marseille, France

Eloi Prud'homme, M.D.
APHM
Marseille, France

Julien Bordes, M.D., M.Sc.
Sainte Anne Military Hospital
Toulon, France
and
Ecole du Val-de-Grâce
Paris, France

Jean-Marie Forel, M.D., Ph.D.
APHM
Marseille, France
and
Aix-Marseille University
Marseille, France

Eric Meaudre, M.D.
Sainte Anne Military Hospital
Toulon, France
and
Ecole du Val-de-Grâce
Paris, France

Laurent Papazian, M.D., Ph.D.
Christophe Guervilly, M.D., Ph.D.
APHM
Marseille, France
and
Aix-Marseille University
Marseille, France

*Corresponding author (e-mail: pierre.esnault@gmail.com).

References

1. Zhu N, Zhang D, Wang W, Li X, Yang B, Song J, *et al*. A novel coronavirus from patients with pneumonia in China, 2019. *N Engl J Med* 2020;382:727–733.
2. Grasselli G, Zangrillo A, Zanella A, Antonelli M, Cabrini L, Castelli A, *et al*.; COVID-19 Lombardy ICU Network. Baseline characteristics and outcomes of 1591 patients infected with SARS-CoV-2 admitted to ICUs of the Lombardy region, Italy. *JAMA* 2020;323: 1574–1581.
3. Bertoni M, Spadaro S, Goligher EC. Monitoring patient respiratory effort during mechanical ventilation: lung and diaphragm-protective ventilation. *Crit Care* 2020;24:106–108.
4. Brochard L, Slutsky A, Pesenti A. Mechanical ventilation to minimize progression of lung injury in acute respiratory failure. *Am J Respir Crit Care Med* 2017;195:438–442.
5. Telias I, Damiani F, Brochard L. The airway occlusion pressure ($P_{0.1}$) to monitor respiratory drive during mechanical ventilation: increasing awareness of a not-so-new problem. *Intensive Care Med* 2018;44: 1532–1535.
6. Bertoni M, Telias I, Urner M, Long M, Del Sorbo L, Fan E, *et al*. A novel non-invasive method to detect excessively high respiratory effort and dynamic transpulmonary driving pressure during mechanical ventilation. *Crit Care* 2019;23:346.
7. Gattinoni L, Chiumello D, Caironi P, Busana M, Romitti F, Brazzi L, *et al*. COVID-19 pneumonia: different respiratory treatments for different phenotypes? *Intensive Care Med* 2020;46: 1099–1102.
8. Beloncle F, Piquilloud L, Olivier P-Y, Vuillermoz A, Yvin E, Mercat A, *et al*. Accuracy of P0.1 measurements performed by ICU ventilators: a bench study. *Ann Intensive Care* 2019;9:104–109.
9. Telias I, Junhasavasdikul D, Rittayamai N, Piquilloud L, Chen L, Ferguson ND, *et al*. Airway occlusion pressure as an estimate of respiratory drive and inspiratory effort during assisted ventilation. *Am J Respir Crit Care Med* 2020;201: 1086–1098.
10. Umbrello M, Fumagalli J, Pesenti A, Chiumello D. Pathophysiology and management of acute respiratory distress syndrome in obese patients. *Semin Respir Crit Care Med* 2019;40: 40–56.

11. Spinelli E, Mauri T, Beitler JR, Pesenti A, Brodie D. Respiratory drive in the acute respiratory distress syndrome: pathophysiology, monitoring, and therapeutic interventions. *Intensive Care Med* 2020; 46:606–618.

Injury to the Endothelial Glycocalyx in Critically Ill Patients with COVID-19

To the Editor:

Severe acute respiratory syndrome coronavirus 2 (SARS-CoV-2) causes the so-called coronavirus disease (COVID-19), which is characterized by a broad spectrum of clinical presentations ranging from asymptomatic patients to critically ill individuals with a high case fatality rate (1). The critical care community has increasingly recognized that cardiovascular and thrombotic complications are relatively common in COVID-19 (2). Indeed, direct involvement of the vascular endothelium was recently reported in a series of patients suffering from severe COVID-19 (3). The endothelial glycocalyx (eGC), which covers the luminal surface of endothelial cells, contributes to the maintenance of vascular homeostasis, whereas disruption of the eGC is observed early in critically ill patients and is associated with inferior outcomes (4, 5).

Here, we investigated in translational human and cellular studies whether injury to the eGC can be found in critically ill patients with COVID-19 early after admission to the ICU. We collected plasma and serum from 19 adult individuals within 24 hours after invasive ventilation for acute respiratory distress syndrome and from 10 healthy human donors after written informed consent of patients or their legal representative. The first patient was admitted on March 19, 2020, and the observation period was until May 17, 2020. The median (interquartile range) observation duration was 47 (40–54) days.

Baseline patient characteristics at study inclusion as well as a description of the further clinical course are summarized in Table 1. Organ failure was not restricted to the lungs, and multiorgan dysfunction was common both at inclusion and during the further clinical course. Surprisingly, global markers of endothelial injury such as Angpt-1 (angiopoietin-1) (control: 29 [26.2–30.9] ng/ml vs. COVID-19: 27.8 [23.4–36.2] ng/ml; $P = 0.79$) and Angpt-2 (control: 0.655 [0.336–1.113] ng/ml vs. COVID-19: 0.434 [0.035–1.338] ng/ml; $P = 0.6$) were unchanged in patients with COVID-19. In contrast, marked increases in the soluble form of the sTie2 (Tie2 receptor) (Figure 1A) and in syndecan-1 (Figure 1B)—indicating pathological shedding of transmembrane proteins involved in glycocalyx structure and processing—were observed. The key eGC sheddase Hpa-1 (heparanase-1) and its enzymatic activity were both not significantly increased (data not shown). To the contrary, the Hpa-1 counterpart, the protective Hpa-2 (heparanase-2), was pertinently reduced in all patients with COVID-19 (Figure 1C). Driven by this acquired Hpa-2 deficiency, the Hpa-1:Hpa-2 ratio was higher in patients with COVID-19 ($P = 0.012$; data not shown). Together, this indicates that critically ill patients with COVID-19 suffer from an acquired Hpa-2 deficiency that can contribute to the degradation of the eGC, maybe even before classical endothelial activation and injury. Next, eGC structure was analyzed in humans, employing sublingual sidestream darkfield (SDF) imaging. We quantified the size of the individual patients' eGC using an indirect surrogate termed the perfused boundary region and found a decrease of perfused boundary region, indicating reduced eGC thickness in patients with COVID-19. To demonstrate that the deficiency of Hpa-2 is mechanistically involved in the degradation of the eGC, we used a microfluidic chamber with cultured endothelial cells (ECs) under flow that synthesize an intact and stable eGC under *in vitro* conditions. After stimulation with COVID-19 or control serum, the eGC was visualized by confocal microscopy followed by computerized three-dimensional reconstruction. Its thickness was then quantified by analyzing the heparan sulfate (HS)-positive area. We found that stimulation with COVID-19 was sufficient to severely damage the eGC (Figure 1E). The HS-positive area was reduced by 34% (control: $6.1 \pm 0.9\%$ vs. COVID-19: $4 \pm 0.4\%$ $P < 0.001$). Consistent with our observation in patients, we found that the transcription of Hpa-2 in COVID-19–stimulated ECs was significantly reduced after 6 hours (0.63 ± 0.02 relative expression to control; $P = 0.003$). Of note, transgenic overexpression of Hpa-2 in a lentivirus-transduced EC line was sufficient to reverse this phenotype, as the HS area in COVID-19 serum–treated lenti-control cells was $1.9 \pm 0.6\%$ but was $4.2 \pm 1.2\%$ in lenti-Hpa-2–overexpressing cells ($P < 0.001$). In other words, if ECs overexpress Hpa-2, the serum of patients with COVID-19 cannot degrade the eGC anymore.

This exploratory study has obvious limitations, most importantly, its small sample size and hypothesis-generating nature. Injury to the eGC is not a finding specific for COVID-19 but can be found in a wide range of critically ill patients (5). Because only a small selection of molecules that may participate in endothelial injury have been investigated in this study, we cannot exclude that further mediators may play a critical role in endothelial and eGC injury in patients with COVID-19. In addition, because of concerns of viral transmission, SDF imaging values could not be obtained from the same control patients from whom blood analysis was performed but were obtained from a separate historic in-center control cohort. Both control cohorts were not matched to the individual patients in terms of age, but the control group that blood was collected from was matched in terms of male predominance.

In summary, we found injury of the eGC and speculate that this might represent a potentially critical hallmark of later widespread endothelial injury in severe COVID-19. Reduced eGC thickness was visualized *in vivo* by employing sublingual SDF imaging in patients. At the same time, increased syndecan-1 and sTie-2 concentrations in the blood of these patients indicated shedding of important

S.D. is supported by the German Research Foundation (DA 1209/4-3) and the German Center for Lung Research.

Authors Contributions: K.S., P.A.G., B.S., T.W., H.H., M.M.H., and S.D. obtained retrospective data. K.S., P.A.G., A.B., and S.D. performed sidestream darkfield imaging measurements. P.A.G. and T.P. performed ELISA measurements, and Y.K. performed and analyzed flow measurements. K.S., P.A.G., H.H., T.W., M.M.H., and S.D. analyzed and discussed the data and generated figures and tables. K.S., P.A.G., and S.D. wrote the manuscript; all authors proofread the manuscript.

Originally Published in Press as DOI: 10.1164/rccm.202007-2676LE on August 24, 2020